Progress In Electromagnetics Research M, Vol. 96, 55–67, 2020

Auxiliary Antenna Array Analysis and Design for Sidelobe Interference Cancellation of Satellite Communication System

Qiliang Wang, Yi Li, Kang Luo*, Qing Wang, Fangmin He, and Bin Li

Abstract—An auxiliary antenna array scheme for sidelobe interference cancellation of satellite communication system is proposed in this paper. Considering earth curvature, signal bandwidth, and transmission loss, a precise model of satellite communication interference scenario is established. In order to improve anti-interference capability, the performance of the auxiliary antenna array is studied by the minimum mean square error (MMSE) criterion. Then, a 7-unit linear microstrip antenna array is manufactured as the auxiliary antenna array. The main contribution of this paper is the corresponding auxiliary antenna array analysis and design. Simulated and experimental results confirm that the proposed scheme can achieve a relatively high interference cancellation radio (ICR) of about 25 dB in a wide beam range.

1. INTRODUCTION

Satellite communication is widely used in practice of application like business, meteorology, and agriculture [1]. Since satellite usually has to transmit and receive signals over long distance, satellite antennas usually have high gain with wide sidelobe coverage, which means that there is always various interference signal entering from sidelobes [2]. If the power of interference signal is much higher than that of the communication signal, the performance of satellite communication will be interfered. Therefore, the satellite system needs to have an ability to adaptively resist sidelobe interference.

There are mainly two types of method, i.e., ultra-low sidelobe technologies and sidelobe cancellation (SLC) technologies, to suppress sidelobe interference [3]. Ultra-low sidelobe technologies suppress interference by reducing the level of entire sidelobes. They are effective but complex and costly, even with regard to the large loss of resolution. Instead, SLC technologies can form desirable nulling in the direction of interference when using a few auxiliary antennas, which is more economical and efficient [4–6].

SLC technologies have been applied in satellite communication system [7–11]. In 1984, Toshiyuki et al. first used adaptive SLC technologies to suppress the interference of earth station [7]. A new interference cancellation system was devised between satellite and terrestrial communications system, and the interference cancellation radio (ICR) of 30 dB is realized. Byounghak et al. use digital channelizer method to improve the efficiency of interference cancellation [8]. However, the performance of technology is usually analyzed by signal simulation, while the radiation field of antenna is neglected. The principle of SLC is to generate a cancellation signal that has opposite phase and equal amplitude of the interference signal, and then add the cancellation signal with the interference signal to suppress the interference [7]. Therefore, as the signal input/output terminal, the electromagnetic performance and layout of antenna need to meet the SLC requirement.

Received 15 July 2020, Accepted 18 August 2020, Scheduled 4 September 2020
* Corresponding author: Kang Luo (luokang89@163.com).
The authors are with the National Key Laboratory of Science and Technology on Vessel Integrated Power System, Naval University of Engineering, Wuhan, Hubei 430033, China.

Interference cancellation requirements are usually estimated by establishing a satellite communication scenario. There are studies for satellite communication interference suppression based on distinctive interference scenarios [9–11]. However, most of the scenarios mentioned above are vague based on many ideal assumptions, which cannot guarantee the accuracy of the interference cancellation requirement. Besides, the performance of antenna is not fully considered. Hence, to conduct sufficient interference cancellation, we propose an auxiliary antenna array scheme and design an independent 7-unit auxiliary antenna array with a simple structure and excellent performance. We analyze the performance of auxiliary antenna array gain, beamwidth, and the array layout. The analysis data of antenna pattern are exported from commercial electromagnetic simulation software instead of ideal antenna model. The simulated and experimental results comply well with each other which verify the effectiveness of the proposed scheme. Simulation results are compared with those of some similar structures (Table 1). Most literatures analyze the interference suppression performance of auxiliary antenna array based on theoretical antenna models by simulation with the lack of experimental results. The proposed antenna array scheme obtains an average ICR about 30 dB in the range of $-90^\circ \sim 90^\circ$ by simulation. Additionally, we fabricate the proposed auxiliary antenna array and conduct a satellite interference cancellation experiment. Experimental results confirm that the proposed scheme can achieve a relatively high ICR about 22–27 dB in the sidelobe range.

Table 1. Comparison of similar structures.

Reference	Algorithm	Antenna structure	Auxiliary element number	Suppression range (deg)	Simulation average ICR (dB)
[11]	LMS	line array	3	$-6 \sim 6$	20
[12]	MSC	line array	3	−20–20	21
[13]	MMSE	line array	6	$-60 \sim 60$	27
[14]	MMSE	square array	16	$-40 \sim 40$	30
[15]	LMS	diagonal array	6	$-8 \sim 8$	19
[16]	DCMP-CN	uniform circular	6	$-80 \sim 80$	24
[17]	DMI	ring array	16	$-9 \sim 9$	26
[18]	LMS	double ring	7	$-90 \sim 90$	20
proposed	MMSE	line array	7	−90–90	30

The remainder of this paper is organized as follows. Section 2 establishes a satellite communication link model. Section 3 presents the SLC algorithm. Section 4 proposes the layout of independent auxiliary antenna array. Section 5 presents the experimental results.

2. SATELLITE COMMUNICATION LINK MODEL AND INTERFERENCE CANCELLATION ANALYSIS

In this section, we first establish the simulated model of satellite antenna and export the radiation pattern by commercial electromagnetic simulation software in Section 2.1. Then, a mathematical model of satellite interference link is proposed in Section 2.2. According to Sections 2.1 and 2.2, the required ICR is obtained in Section 2.3.

2.1. Simulation Model of Satellite Antenna

In order to carry out the integrated simulation and performance analysis of the auxiliary antenna array, the model of the satellite system is set up as shown in Fig. 1. Fig. 1(a) depicts the simulated model of feed antenna, which is a corrugated horn antenna. The integrated simulation model of parabolic

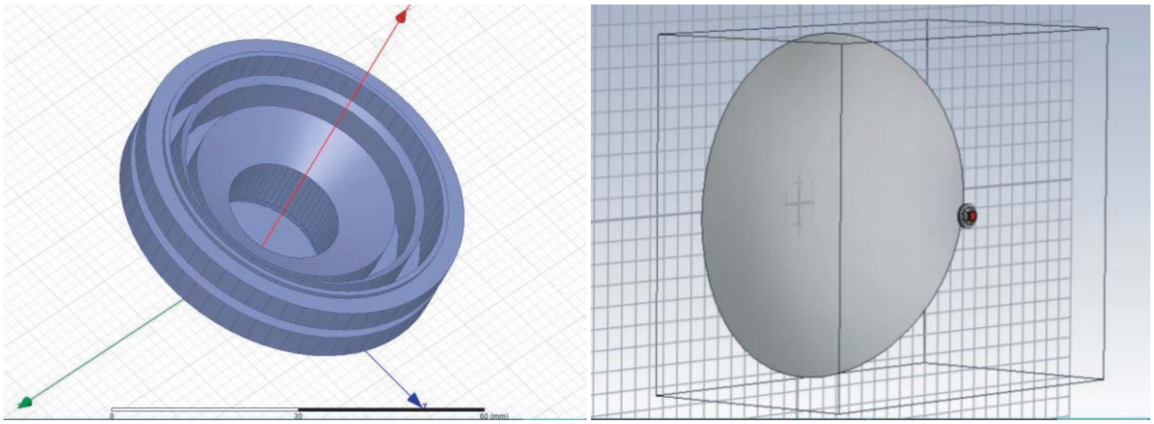

(a) (b)

Figure 1. Simulated model of the satellite antenna. (a) Feed antenna. (b) Satellite antenna.

antenna and feed antenna is established as shown in Fig. 1(b). The fitting formula of parabolic antenna is:

$$Z(x,y) = \frac{\left(x^2+y^2\right)}{4f_0} \tag{1}$$

where the major axis and minor axis are respectively $x = -500 \sim 500\,\text{mm}$ and $y = -400 \sim 400\,\text{mm}$, and the focal distance is $f_0 = 550\,\text{mm}$.

The simulated reflection coefficient is depicted in Fig. 2(a) together with the radiation pattern in Fig. 2(b). It can be observed that the gains of the main lobe and sidelobe are respectively 39.6 dBi and 10 dBi, and the range of 3 dB-beamwidth is $-2° \sim 2°$. The exported radiation pattern will be used to analyze the performance of the auxiliary antenna in Section 4.

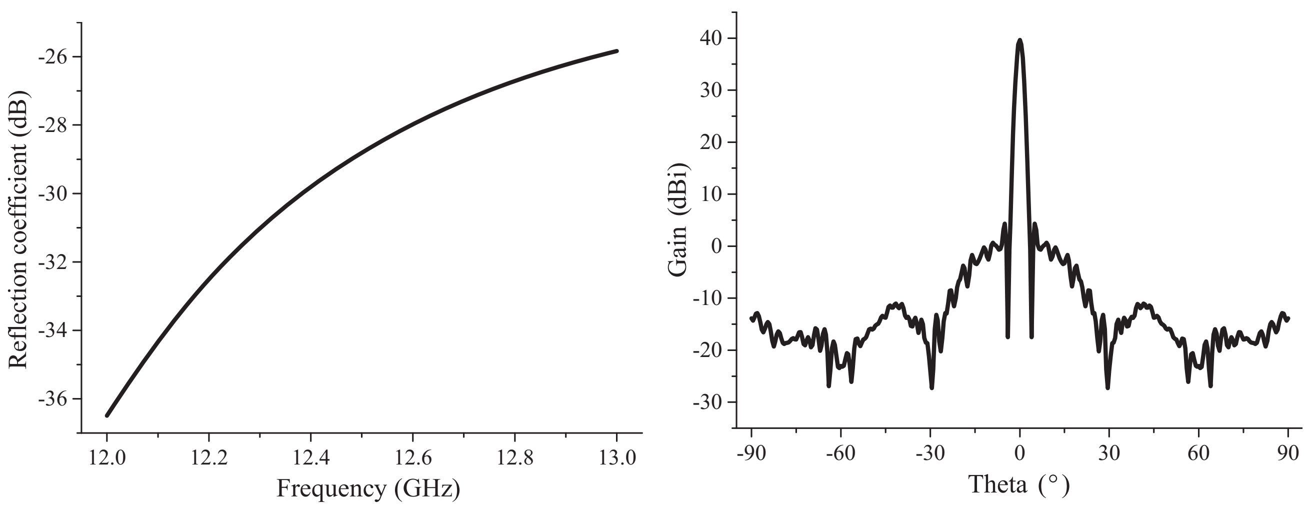

(a) (b)

Figure 2. Simulated results of satellite antenna. (a) Reflection coefficient. (b) Radiation pattern.

2.2. Satellite Communication Link Model

The space relationship diagram of earth station satellite, space station, and interference source are shown in Fig. 3. We assume that the mainbeam of the earth station satellite antenna is always aimed at

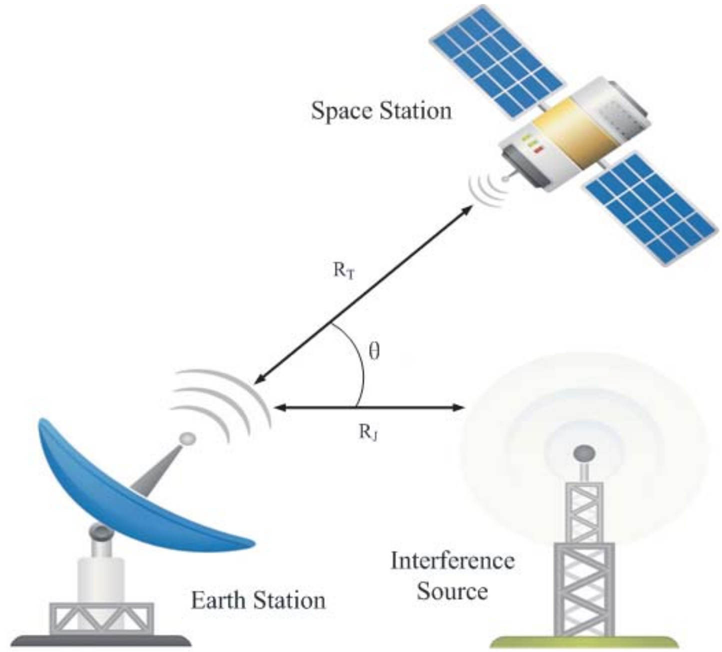

Figure 3. Space relationship diagram of earth station satellite, space station and interference source The interference signal power received by satellite is [24, 25].

the direction of the desired signal, and the interference signal comes from the direction of the sidelobes. The interference signal and the desired signal propagate along a straight line. The signal power of satellite communication can be written as [19, 20]

$$S = G_d + EIRP_R - C - L \tag{2}$$

where $G_d = 39.6\,\text{dBi}$ is the gain of earth station antenna as shown in Fig. 3, $EIRP_R$ the equivalent omni-directional radiated power of space station satellite antenna, $C = 0.1 \sim 0.2\,\text{dB}$ the additional link loss [14], and L the total transmission loss of satellite antenna and space station antenna

$$EIRP_R = G_R + P_R \tag{3}$$

$$L = L_{ad} + L_{pu} + L_d + L_{rd} \tag{4}$$

where G_R is the gain of space station satellite antenna, P_R the output power of the space station satellite, $L_{ad} = 0.2$ the atmospheric attenuation, $L_{pu} = 0.5$ the antenna pointing error, and L_d the transmission loss of satellite antenna and space station antenna in free space [21]

$$L_d = 20 \lg \frac{40\pi R_T f}{3} = 32 + 20 \lg R_T + 20 \lg f \tag{5}$$

where f is the frequency of transmission signal chosen as Ku frequency band, and $R_T = 36000 \sim 42000\,\text{km}$ is the linear distance between satellite and earth station by considering earth curvature

$$R_T = 42238 \cdot \sqrt{1.023 - 0.302 \cos\theta \cos\varphi} \tag{6}$$

where θ is the latitude difference between earth station and geostationary satellite orbit, φ the longitude difference between earth station and geostationary satellite orbit, and L_{rd} the rain area attenuation

$$L_{rd} = aR_p^b \cdot \gamma_p \frac{(H_p - H_0)}{\sin E_a} \tag{7}$$

where $aR_p^b = 0.5$ is the attenuation per unit length of rain area (dB/km), and γ_p is reduction factor [22, 23]

$$\gamma_p = 90 \Big/ \left(90 + 4 \cdot \frac{H_p - H_0}{\sin E_a} \cos E_a\right) \tag{8}$$

where H_p is the height of the zero-degree isotherm of the earth station, H_0 the altitude of earth station, and E_a elevation angle of satellite antenna.

$$J = EIPR_J + G_{RJ}(\theta) - L_J \tag{9}$$

where $G_{RJ}(\theta) = -20 \sim 10\,\text{dBi}$ is the gain of the earth station satellite antenna in the direction of interference as shown in Fig. 3. $EIPR_J$ is the equivalent omnidirectional radiated power of interference source, and L_J is the transmission loss of the interference signal in free space

$$EIPR_J = P_J + 10\lg\frac{B_S}{B_J} + G_J \tag{10}$$

$$L_J = 20\lg\frac{40\pi R_J F}{3} = 32.4 + 20\lg R_J + 20\lg F \tag{11}$$

where P_J is the output power of the interference source, B_S the bandwidth of the desired signal, B_J the bandwidth of the interference signal, G_J the gain of interference source antenna [25], R_J the linear distance between the interference source and the earth station [26], and F the frequency of the interference signal.

Based on the above analysis, Eq. (9) can be rewritten as

$$J = -32 + EIPR_J - 20\lg R_J - 20\lg F + G_{RJ}(\theta) \tag{12}$$

2.3. Interference Cancellation Ratio Calculation

According to [12–19], the major model parameters of satellite link are described in Table 2.

Table 2. Satellite Link model parameters.

Parameters	$EIRP_R$ [20]	G_d	L [23–25]	$G_{RJ}(\theta)$	L_J [25]	R_J [25]
Value	$75 \sim 86$ dBm	39.6 dBi	$205.9 \sim 217.5$ dB	$0 \sim 25$ dBi	157 dB $\sim$ 161 dB	400 km

Substituting the above parameters into Eqs. (2) and (9), the communication signal power received by the satellite can be obtained as -110 dBm ~ -92 dBm, and the interference signal power received by the satellite is -96 dBm ~ -77 dBm. Based on the above analysis, the required ICR range of antenna sidelobes needs to reach 33 dB. The obtained signal power will be used to conduct simulations and experiments in Sections 4 and 5.

3. INTERFERENCE CANCELLATION ALGORITHM

In this section, we present the algorithm for interference cancellation with a main antenna and an auxiliary antenna array. The MMSE criterion is used to optimize the performance of auxiliary antenna array. We summarize the required ICR by calculating the signal interference noise radio (SINR) before and after interference cancellation.

The signal received by the main antenna is [27]

$$X_M = (S + C) \times P_M + N_M \tag{13}$$

The signal received by the auxiliary antenna is

$$X_A = (S + C) \times P_A + N_A \tag{14}$$

where S is the desired signal; C is the interference signal; P_M is the pattern exported from Fig. 2(b); N_M and N_A are respectively the noise signal received by main antenna and auxiliary antenna; P_A is calculated as

$$P_A(\theta) = \sum_{n=0}^{N-1} \mathrm{G}_n(\theta) e^{j(\varphi_n + (2\pi/\lambda) nd \sin\theta)} = \sum_{n=0}^{N-1} \mathrm{G}_n(\theta) e^{j(2\pi/\lambda) nd(\sin\theta - \sin\sigma)} \tag{15}$$

The weight of main antenna W_q is given as a constant, and the weight of auxiliary antenna is

$$W_{opt} = R_{C,A}^{-1} R_{C,A-M} W_q \tag{16}$$

where $R_{C,A}$ is the covariance matrix of additional noise interfering signals received by the auxiliary array, and $R_{C,A-M}$ is the covariance matrix of additional noise interfering signals received by main array and auxiliary array

$$R_{C,A} = E\left((S_A + C_A + N_A)(S_A + C_A + N_A)^H\right) \tag{17}$$

$$R_{C,A-M} = E\left((S_A + C_A + N_A)(S_M + C_M + N_M)^H\right) \tag{18}$$

The SINR before interference cancellation is

$$SINR_{bef} = \frac{S_M^2}{(C_M + N_M)^2} \tag{19}$$

The SINR after interference cancellation is

$$SINR_{aft} = \frac{(S_M - W_{opt} S_A)^2}{(C_M + N_M - W_{opt}(C_A + N_A))^2} \tag{20}$$

We then define the ICR as

$$ICR = \frac{SINR_{aft}}{SINR_{bef}} = \frac{(C_M + N_M)^2}{(C_M + N_M - W_{opt}(C_A + N_A))^2} \tag{21}$$

According to the above analysis, we can establish a relationship among the signals, antenna patterns, and ICR by adaptive algorithm mentioned above, which will be used to analyze the performance of auxiliary antenna in Section 4.

4. AUXILIARY ANTENNA PERFORMANCE ANALYSIS

In this section, the number of antenna array units, gain, and beamwidth of auxiliary antenna pattern are obtained by using the method of functions fitting. In addition, we discuss the performance of two auxiliary antenna layouts. The analytical results show that the ICR ranges of the single row and the double row are respectively 10–40 dB and 23–37 dB. Finally, the single row antenna layout is chosen to conduct subsequent interference suppression experiment in Section 5.

4.1. Auxiliary Antenna Array Analysis

In order to suppress sidelobe interference, it is necessary to ensure that the gain of auxiliary antenna array is higher than sidelobe gain of main antenna (10 dBi) [28]. The empirical formula of maximum gain of antenna array is [29]

$$G_m = G_u + 10 \lg N \tag{22}$$

where G_u and N are respectively the gain and number of the auxiliary antenna units. The gain of conventional rectangle microstrip patch antenna is generally about 6 dBi. Consequently, N is selected as 7 in this paper. According to multi-saturation interference cancellation principle [30], the 7-unit antenna array can suppress six interference sources at the same time. Fig. 4 presents the original main antenna pattern and the pattern after interference cancellation, which form zero traps at $\pm 10°$, $\pm 25°$, and $\pm 40°$, respectively. Since the unit gain is inversely proportional to the square of the beamwidth, we construct three parabola functions to study the influence of gain and beamwidth on interference suppression as shown in Fig. 5. The maximum gains of Aux. 1–3 are respectively 10 dBi, 7 dBi, and 4 dBi. Meanwhile, the beamwidths of Aux. 1–3 are respectively 61°, 73°, and 92°.

We assume that the noise is white noise which is uncorrelated with other signals. The range of signal power is given in Section 2.3. The desired signal with SNR of -140 dB comes from the mainlobe direction (0°), and the interference signal with INR of -107 dB comes from the direction ($-90° \sim 90°$). Fig. 6 shows the interference suppression performances of three auxiliary antenna patterns. It can be seen that a higher gain of interference direction will lead to a deeper nulling. Considering the depth of the nulling and the coverage of pattern comprehensively, the fitting pattern of Aux. 2 is selected as the reference of auxiliary antenna.

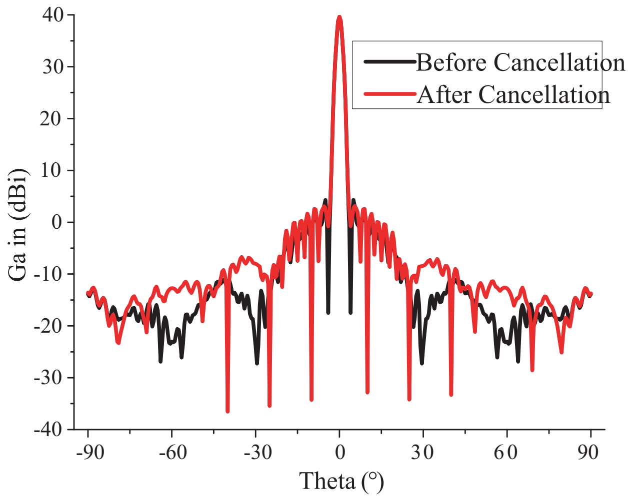

Figure 4. The interference suppression effect for six interference source.

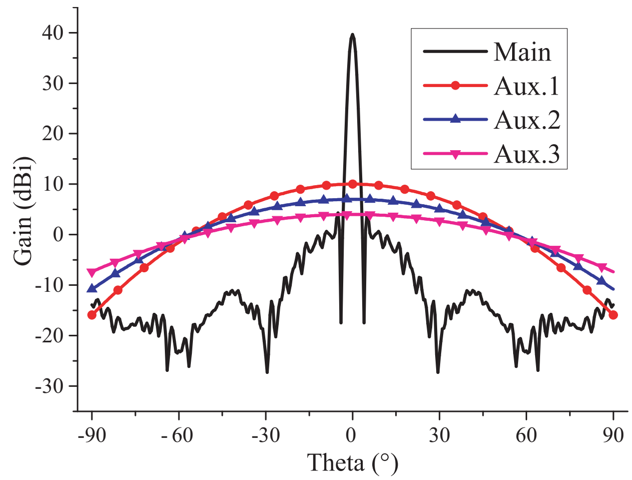

Figure 5. The auxiliary antenna unit patterns with different fitting functions.

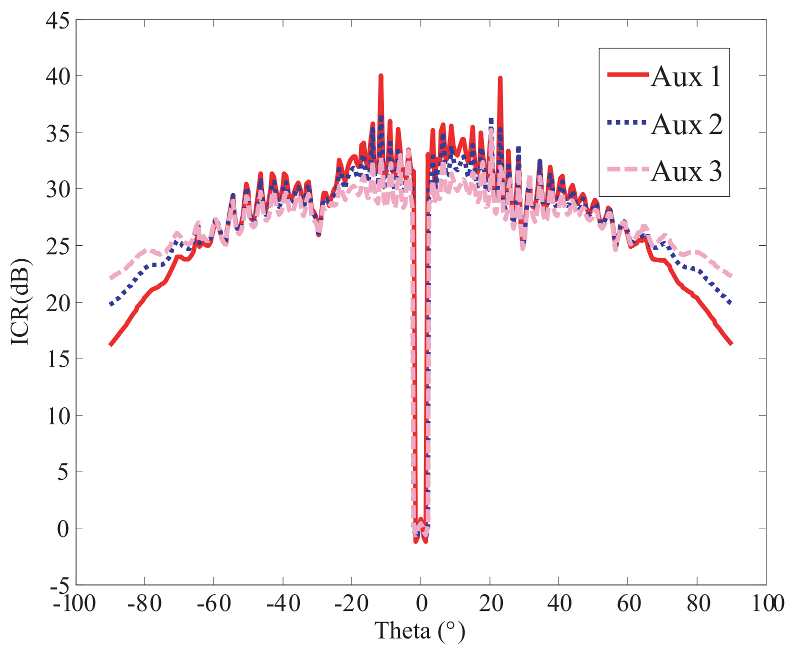

Figure 6. The interference suppression performance of the fitting patterns in Fig. 5.

4.2. Auxiliary Antenna Array Layout Analysis

The layouts of auxiliary antenna and main antenna are shown in Fig. 7. The distance between the main antenna and the auxiliary antenna array is $D = 0.5\,\text{m}$. For the single row layout, the array units are equally spaced with an interval of about half a wavelength ($d = 0.012\,\text{m}$). For the double row layout, the units of the upper and lower rows are cross symmetric. The interval between the two rows is $dy = 0.027\,\text{m}$, and the array units in each row are equally spaced with an interval of $dx = 0.1\,\text{m}$.

When the weight value is 1, the patterns of the two auxiliary antenna arrays are shown in Fig. 8. It can be seen that the maximum gain of the single row layout is 14.6 dBi, and there are undesired gate lobes in the double row layout with the maximum gain of 15.2 dBi.

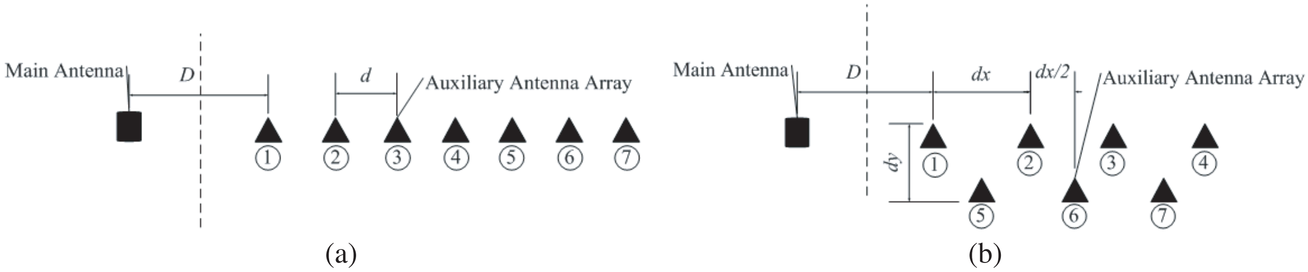

Figure 7. The layout of auxiliary antenna and main antenna. (a) Single row. (b) Double rows.

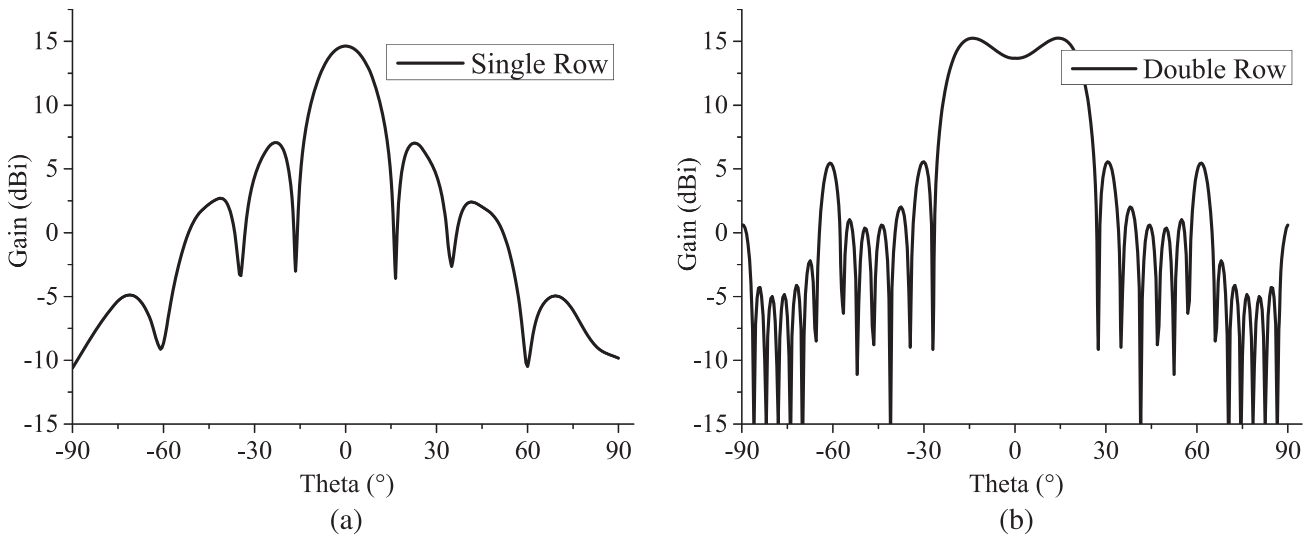

Figure 8. The pattern of two auxiliary antenna arrays. (a) Single row. (b) Double row.

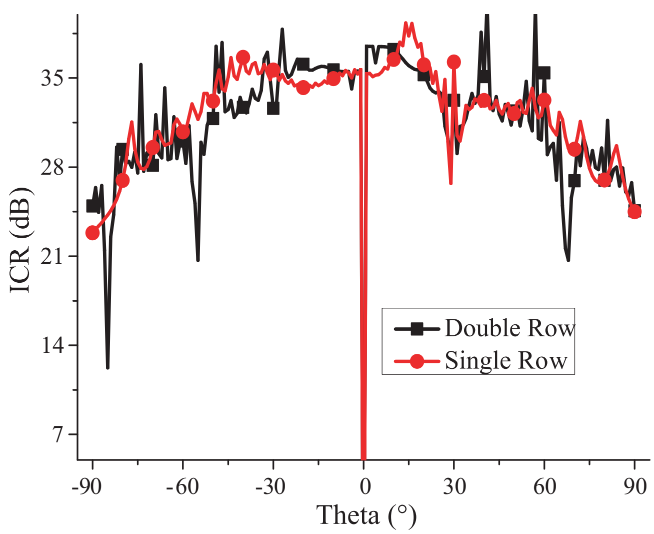

Figure 9. The ICR of two auxiliary antenna array layouts.

Figure 9 shows the ICR of two auxiliary antenna array layouts with different angles. It can be observed that the ICR decreases with the increase of interference angle. In fact, the increase in angle means the decrease in gain. Therefore, the ICR is proportional to the sidelobe level. Since the mainlobe of the antenna always points to the direction of the desired signal, when the interference signal comes from the direction of the mainlobe, the desired signal will also be suppressed. Such being the case, the ICR is very low in the mainlobe range. In the sidelobe range, the ICR range of double rows is 10–40 dB, and that of single row is 23–37 dB. Obviously, the interference suppression effect of single row is more stable, and it is finally selected to suppress interference.

5. EXPERIMENT RESULTS

In this section, we first fabricate and test the proposed auxiliary antenna layout of a 7-unit linear array. Then, we establish a satellite interference cancellation experiment system. Experimental results confirm that the proposed scheme can achieve the required ICR in the sidelobe range.

In order to estimate the cancellation performance of interference suppression in actual working conditions, experiments are conducted using the designed auxiliary antenna array. The satellite interference cancellation system is shown in Fig. 10. It has the following components: two satellite antennas which are used to transmit and receive signals respectively, the sampling module where the auxiliary antenna array is installed to receive the interference signal, the cancellation module which modifies the amplitude and phase of the interference signal received by the auxiliary antenna array. Moreover, we select a horn antenna as the interference source, and the power of the interference signal can be adjusted by changing the transmit power and the distance between the horn and interference cancellation system. The auxiliary antenna array is shown in Fig. 11(a), which is fixed to the rear metal plate of the sampling module by wall SMA joint. After installation, the measured reflection coefficient is shown in Fig. 11(b).

The auxiliary antenna and satellite antenna are equipped with a down-conversion module at their rear ends. Hence, the desired signal and the signal before and after cancellation are processed at the intermediate frequency band instead of Ku. The spectrum of the desired signal is depicted in Fig. 12. Four experimental results of the signal spectrum before and after cancellation are given in Fig. 13. It can be observed that the signal spectrum after interference cancellation is similar to that of the desired signal. Due to the existence of internal noise in the system, the entire spectrum of signal is slightly

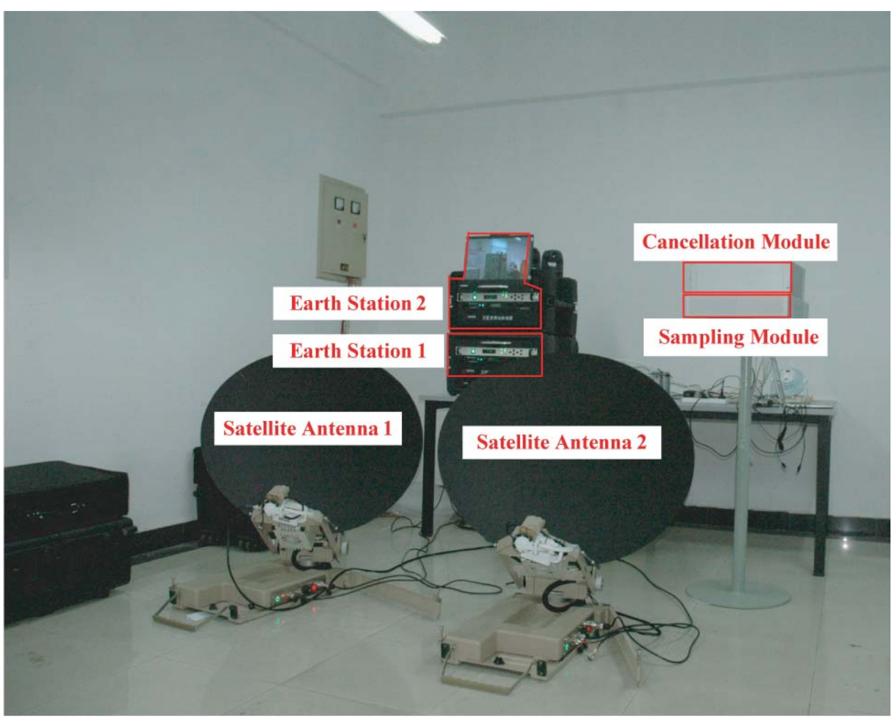

Figure 10. Satellite interference cancellation experiment system.

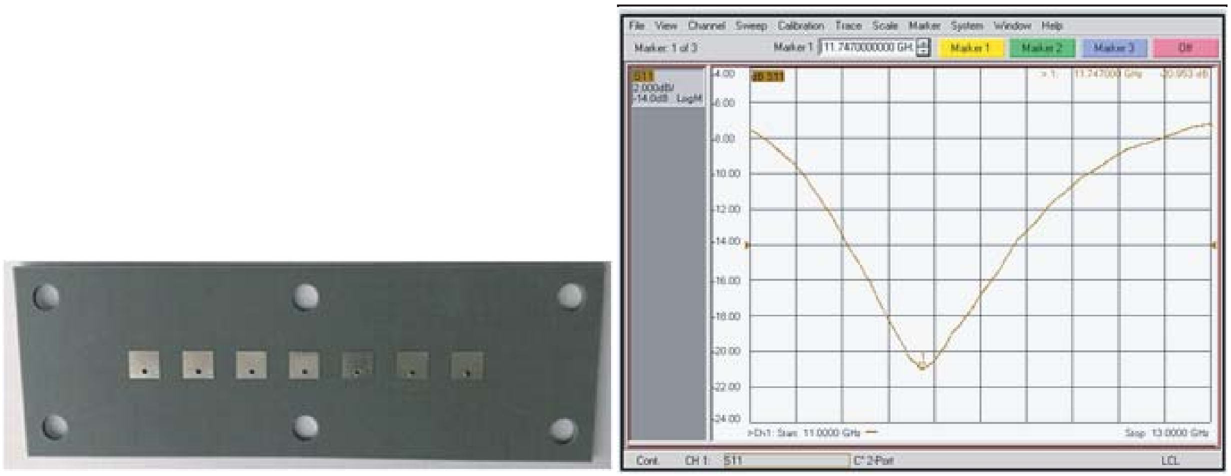

(a) (b)

Figure 11. The fabricated and tested results of a 7-unit linear auxiliary antenna array. (a) Fabricated antenna. (b) Reflection coefficient.

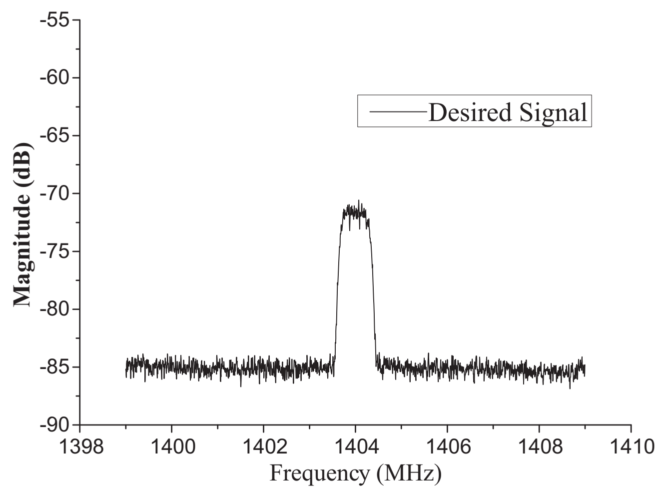

Figure 12. Spectrum of the desired signal.

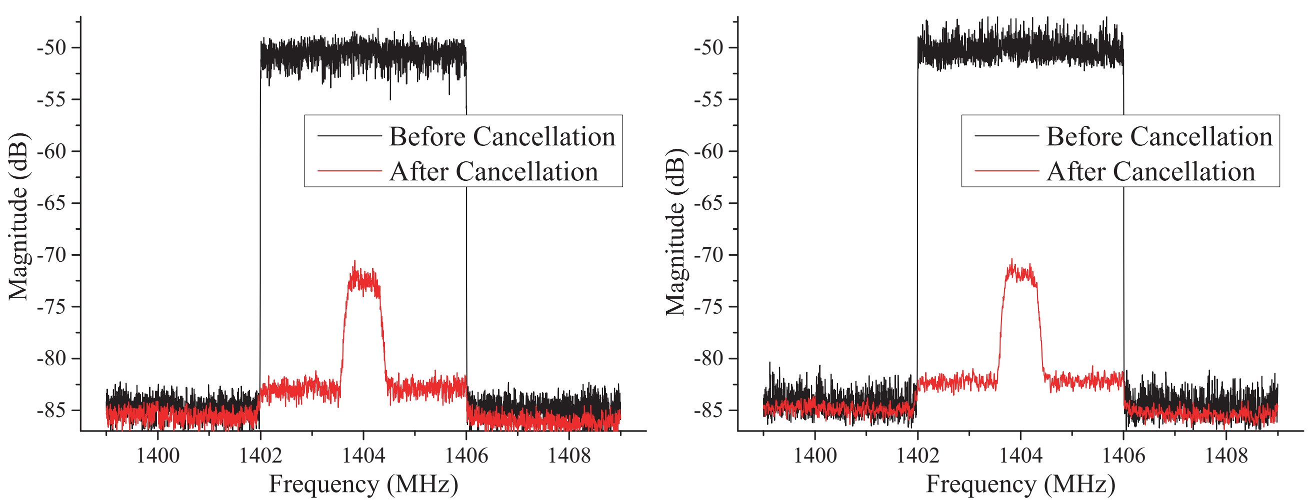

(a) (b)

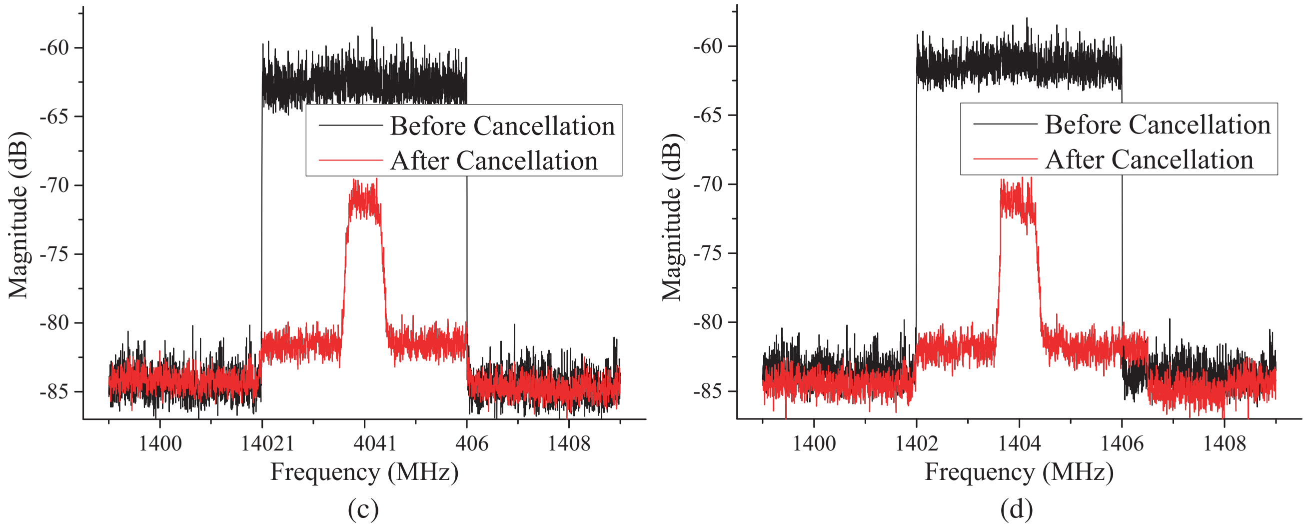

Figure 13. Spectrum of the signal before and after cancellation. (a) Interference suppression at $-3°$. (b) Interference suppression at $+3°$. (c) Interference suppression at $-85°$. (d) Interference suppression at $+85°$.

raised. The ICR at $-3°$, $+3°$, $-85°$, and $+85°$ are 27 dB, 26 dB, 23 dB, and 22 dB, respectively. Due to the influence of signal transmission loss and fabricated error in the experimental system, the actual ICR ($22 \sim 27$ dB) is slightly lower than the required ICR (33 dB).

6. CONCLUSIONS

In this paper, an auxiliary antenna array scheme for satellite communication system interference cancellation application is proposed. The interference cancellation requirement (33 dB) is estimated by establishing a precise satellite link model. The influence of auxiliary antenna performance on interference suppression is analyzed, and the characteristic parameters of the auxiliary antenna array are obtained. In addition, two antenna layouts are compared by using the proposed scheme, and the layout of single row is finally fabricated and tested due to the stable performance. Experimental results confirm that the proposed scheme achieves a relatively high ICR of about 22–27 dB in the sidelobe range, which can be applied to optimize the interference suppression performance in other satellite communication systems.

ACKNOWLEDGMENT

This work is partially supported by the Natural Science Foundation of Hubei Province under Grant ZMRS2019001636 and Grant 2019CFB257.

REFERENCES

1. Pan, Z., "Talking about the adjustment of Ku-band satellite system on-line and signal transmission process," *Science and Technology Vision*, 23–24, Nov. 2017.
2. Pan, G., *Anti-jamming Technology of Satellite Navigation Receiver*, 322–325, Electronic Industry Press, May 2016.
3. Naik, K. and K. Raju, "Synthesis of linear concentric ring arrays with high directivity and low sidelobe levels," *Wireless Personal Communications*, Vol. 87, No. 12, 1–15, Aug. 2016.
4. Zhao, S., "Research on sidelobe cancellation technology of beidou navigation receiver," Nanjing University of Posts and Telecommunications, May 2017.

5. Howells, P. W., "Intermediate frequency sidelobe canceller," U.S.Patent3202990, Aug. 1965.
6. Mohammed, J. R. and K. H. Sayidmarie, "Performance evaluation of theadaptive sidelobe canceller system with various auxiliary configurations," *AEU — International Journal of Electronics and Communications*, Vol. 80, 179–185, Aug. 2017.
7. Toshiyuki, K., et al., "Interference cancellation system for satellite communication earth station," *IEEE Transactions on Communications*, Vol. 32, No. 7, 796–803, Jul. 1984.
8. Byounghak, K., H. Yu, and S. Noh, "Cognitive interference cancellation with digital channelizer for satellite communication," *Sensor*, Vol. 20, No. 2, 355, May 2020.
9. Xu, R. Y., "Self-Interference cancellation scheme for secure AF satellite communication based on FH-MWFRFT," *IEEE Communications Letters*, Vol. 23, No. 11, 2050–2053, Sep. 2019.
10. Manlio, B., "Diversity framed slotted aloha with interference cancellation for maritime satellite communications," *ICC 2019 — 2019 IEEE International Conference on Communications (ICC)*, Shanghai, China, May 2019.
11. Liu, Y. P. and L. P. Wang, "Adaptive wideband sidelobe cancellation based on uniform line array," *IEEE Transactions on Communications*, Vol. 12, No. 3, 130–133, Apr. 2012.
12. Jeffs, D. and K. Warnick, "Improved interference cancellation in synthesis array radio astronomy using auxiliary antennas," *International Conference on Acoustics, Speech and Signal Processing (ICASSP)*, 2003.
13. Mohammed, J. and K. Sayidmarie, "Performance evaluation of the adaptive sidelobe canceller system with various auxiliary configurations," *International Journal of Electronics and Communications (AEÜ)*, 179–185, Jun. 2017.
14. Liao, K., "Novel antenna array synthesis methods and adaptive sidelobe cancellation algorithms," Xiamen University, Xiamen, Jun. 2014.
15. Wang, B., "Design and research of satellite anti-jamming device based on sidelobe cancellation technology," University of Electronic Science and Technology of China, Chengdu, May 2012.
16. Kamio, K. and T. Sato, "An adaptive sidelobe cancellation algorithm for high-gain antenna arrays," *Electronics and Communications in Japan Part 1*, Vol. 87, No. 3, 11–18, 2004.
17. Yang, R., "Algorithms of sidelobe cancellation and mainlobe jamming cancellation by polarization for array antenna," Xidian University, Xi'an, Jan. 2012.
18. Byun, G., S. Kim, and H. Choo, "Optimum array configuration to improve the nullsteering performance for CRPA systems," *Proceedings of ISAP*, Dec. 2014.
19. Li, Z., "Ku-band satellite communication link calculation," *Communication Technology*, Vol. 48, No. 6, Naval University of Engineering, Jun. 2015.
20. Guan, Y., H. Y. Zhang, and R. Zhong, "Research on calculation model of satellite communication link under interference conditions," *Communication Technology*, Vol. 51, No. 10, 2279–2286, Oct. 2018.
21. Wang, L., "Zhongwei 1' communication satellite," *Satellite and Network*, Vol. 1, No. 3, 51–52, Jun. 2007.
22. Wen, B. P., et al., "Calculation and analysis of satellite transmission system links," *Journal of China Three Gorges University: Natural Science Edition*, Vol. 33, No. 3, 39-42ITU, Mar. 2011.
23. Smith, K., "Centimeter and millimeter wave attenuation and brightness temperature due to atmospheric oxygen and water vapor," *Radio Science*, Vol. 17, No. 6, 1455–1464, Nov. 1982.
24. Wei, Y., "Satellite communication link calculation," *Command Information System and Technology*, Vol. 1, No. 5, 73–76, Oct. 2014.
25. Yong, J. S., "Calculation of microwave interference to C-band satellite receiving station and anti-jamming measures," *Industrial Technology*, No. 24, May 2009.
26. Tian, X. C., "A review of research on satellite communication radio wave propagation," *Railway Communication Signals*, 6–8, Aug. 1988.
27. Ling, Y. D. and Y. L. Wang, "Least squares algorithm using adaptive processing of single snapshot data," *Journal of Huazhong University of Science and Technology (Natural Science Edition)*, Vol. 37, No. 22–24, May 2009.

28. Long, S. M., S. R. Pen, and H. Y. Tang, "Analysis and comparison of adaptive sidelobe cancellation system interference methods," *Electronic Information Countermeasure Technology*, Vol. 31, No. 1, 38–42, Jan. 2016.
29. Lei, D., "Research on microstrip array antenna," Harbin University of Technology, Harbin, Mar. 2016.
30. Hu, S. L., "Research on the technology of radar sidelobe cancellation of multi-directional saturated jamming," *Modern Defense Technology*, Vol. 42, No. 3, 25–30, May 2014.